Letters in Applied NanoBioScience
Open-Access Journal (ISSN: 2284-6808)

Article
Volume 13, Issue 1, 2024, 15
https://doi.org/10.33263/LIANBS131.015

Surface-engineered Oral Sub-micron Particles and Topical Microgels Matrixed with Transcutol-HP/*Capra hircus* Composite for Amplification of Piroxicam Delivery and Anti-inflammatory Activity

Petra Nnamani [1,2,3,4], Franklin Kenechukwu [1,*], Chisom Okoye [1], Anthony Attama [1]

[1] Drug Delivery and Nanomedicines Research Group, Department of Pharmaceutics, Faculty of Pharmaceutical Sciences, University of Nigeria, Nsukka 410001, Enugu State, Nigeria; petra.nnamani@unn.edu.ng and (P.N.); obiomaeze@yahoo.com (P.N.); frankline.kenechukwu@unn.edu.ng (F.K.); chimafrankdiff@yahoo.com (F.K).; chisomokoye100@gmail.com (C.O.); anthony.attama@unn.edu.ng (A.A.); aaattama@yahoo.com (A.A.)
[2] Public Health & Environmental Sustainability Research Group, Department of Pharmaceutics, Faculty of Pharmaceutical Sciences, University of Nigeria, Nsukka 410001, Enugu State, Nigeria; petra.nnamani@unn.edu.ng (P.N.); obiomaeze@yahoo.com (P.N.);
[3] Department of Drug Delivery, HIPS - Helmholtz Institute for Pharmaceutical Research Saarland, Saarbrücken, Germany; petra.nnamani@unn.edu.ng (P.N.); obiomaeze@yahoo.com (P.N.);
[4] Department of Pharmacy, Saarland University, Saarbrücken, Germany.; petra.nnamani@unn.edu.ng (P.N.); obiomaeze@yahoo.com (P.N);
* Correspondence: frankline.kenechukwu@unn.edu.ng (F.K.), chimafrankduff@yahoo.com (F.K.);
Scopus Author ID 55180690700

Received: 1.11.2021; Accepted: 26.08.2022; Published: 11.08.2023

Abstract: Conventional oral and topical piroxicam formulations employed in the treatment of inflammatory conditions are limited by adverse effects and low bioavailability which can be surmounted using lipid-based formulations. The objectives of the study were to comparatively evaluate the physicochemical and pharmacodynamic properties of surface-engineered solid lipid microparticles (SLMs) and microgels of piroxicam designed for oral and topical administration, respectively. Piroxicam (0.2, 0.5, 1.0%w/w) SLMs were formulated using optimized tailor-made Transcutol-HP/*Capra hircus* (CH) lipid-matrix by melt-homogenization, characterized for physicochemical performance, optimized and employed to prepare carbopol-based and poloxamer-based topical microgels. The microgels were evaluated for drug content, physical characteristics, compatibility, viscosity, spreadability, and stability. Thereafter, comparative studies were carried out on the formulations regarding in-vitro drug release and anti-inflammatory activity in rats vis-à-vis the controls. Differential scanning calorimetry (DSC) thermograms showed amorphicity of the lipid-matrix compared with Transcutol-HP/CH, which consequently, led to good encapsulation efficiency (89.16±0.4%) and drug release obtained with SLM containing 0.5%w/w piroxicam. This optimized SLMs also had significantly ($p<0.05$) better anti-inflammatory activity (92±0.7%) than piroxicam (66±0.5%). The microgels showed good physicochemical performance and controlled release potential. Marketed formulation (Roxy® Gel) and carbopol-based microgels gave relatively decreased drug release and exhibited 65.6±0.3% edema inhibition, while poloxamer-based microgel had 67.7±0.2% edema inhibition at 6h. The enhanced anti-inflammatory activity of optimized SLMs and microgels could be attributed to the hydrodynamic sub-micron particles, adequate spreadability, and low viscosity. This study has shown surface-engineered SLMs and microgels as novel oral and topical platforms for amplifying piroxicam delivery and anti-inflammatory activity.

Keywords: microgels; Poloxamer® 407; Carbopol® 974; *Capra hircus*; anti-inflammatory activity.

1. Introduction

Inflammatory disorders are treated primarily with non-steroidal anti-inflammatory drugs (NSAIDs). Piroxicam, an oxicam derivative having an enolic 4-hydroxy substituent and a member of the NSAIDs, acts by inhibiting the synthesis of arachidonate cyclo-oxygenase enzyme (COX) and so causes the inhibition of the production of prostaglandins (a phospholipid of the cell membrane), reduces inflammation [1,2]. Piroxicam thus exhibits pronounced anti-inflammatory, analgesic, and antipyretic effects, and is thus useful in the chronic management of rheumatoid arthritis, ankylosing spondylitis, osteoarthritis, acute musculoskeletal disorder, acute gout, post-operative pain or after acute trauma, and treatment of primary dysmenorrhea in patients of 12 years old and above [3,4].

Meanwhile, a lot of techniques are used to improve the biopharmaceutical and pharmacodynamics of poorly water soluble drugs, including formulation approaches invloving polymeric and lipidic systems [5-24]. The poor aqueous solubility and severity of some adverse effects of piroxicam (e.g., gastrointestinal tract (GIT) ulceration and bleeding) have been reduced through lipid-based formulations [1-3], which are widely used due to the diversity, biocompatibility and versatility of pharmaceutical grade lipid excipients and their compatibility with liquid, semi-solid and solid drugs [25-29]. Owing to the fact that various lipid-based excipients which have unique features can easily be obtained, this makes it possible for these excipients to be easily manipulated and applied in enhancing the bioavailability of poorly water-soluble drugs and in controlling drug release [30-35]. Lipid formulations generally provide increased drug solubilization for water-insoluble drugs owing to the ease of wetting of hydrophobic drug particles in the presence of lipid matrix and the presence of surfactants that promote wetting [36]. Furthermore, lipids are non-adhesive and, therefore, do not adhere to intestinal walls, unlike most polymers, and so present a good matrix for formulating NSAIDS.

Drugs which have intrinsic delivery problems have been formulated into novel lipid-based drug delivery systems (LBDDS) using the concept of solidified reverse micellar delivery systems (SRMDS) [37-43]. This delivery technique utilize the merits of the traditional delivery systems, including controlled and targetted drug release and industrial production of medicines and also circumvents remarkable demerits of SRMDS, especially toxicity and instability problems [5,44-52].

Recently, homolipids and heterolipids have gained renewed interest as pharmaceutical excipients and have been copiously studied for improved delivery of various drugs [53-59]. Homolipids are esters of fatty acids with various alcohols. This study is centered on formulating oral SLMs of piroxicam based on surface-modified homolipids obtained from goat fat (Capra hircus, CH) and subsequent delivery as topical microgels (prepared with polymeric hydrogels: Carbopol® 971 and Poloxamer® 407). Both oral and topical delivery systems (TDS) have been employed to achieve controlled drug release [60-64]. Hydrogels and microgels are potential TDS [65-68]. Hydrogels are cross-linked water-soluble polymers, which are highly swollen but they do not solublize in the surrounding medium [66,67]. On the other hand, microgels are microscopic particles of hydrogels which achieve sustained release by diffusion from a reservoir through a micro-porous membrane into the skin [65,68,69].

To attenuate the low aqueous solubility and gastric ulceration of piroxicam, both oral SLMs and TDS of piroxicam were developed in this investigation using tailor-made lipid-matrix; topical piroxicam microgels based on poloxamer® 407 and Carbopol® 974 respectively were prepared from SLMs containing homolipids obtained from CH and Transcutol®-HP (lipid

base), Solutol® HS-15 (solubiliser), Tween® 80 (surfactant), and Lutrol® F68 (poloxamer® 188) (solubility enhancer). These excipients and SRMDS have been successfully employed in previous studies by our research team to achieve sustained, controlled, and targeted delivery of several drugs via oral and topical routes of administration [44,57-59,65,70,71]. However, there are no literature reports on topical SRMDS of piroxicam and piroxicam-loaded surface-engineered SLM based on CH and Transcutol®-HP.

Consequently, our aim was to formulate oral SLMs and topical microgels of piroxicam using CH and Transcutol®-HP as lipid-base and to compare the anti-inflammatory activity of the formulations with that of unformulated piroxicam and commercial piroxicam gel, respectively. It is expected that the increased surface area of particles making up the formulations would enhance the anti-inflammatory effects of the formulations and possibly delay/prolong the release of piroxicam *vis-a-vis* the commercial piroxicam gel.

2. Experimental

2.1. Materials.

The materials used include: pure piroxicam sample (Juhel Nigeria Limited, Nigeria), Transcutol®-HP (Gattefossé, Saint-Priest Cedex, France), Tween® 80 (Kermel, China), Solutol® HS 15 (Polyoxyl 15 Hydroxystearate, USP/NF), Poloxamer® 407 and Lutrol® F-68 (poloxamer® 188) (BASF, Ludwigshafen, Germany), Carbopol® 974 (Lubrizol Corporation, USA), triethanolamine (Spectrum Corporation, USA), dialysis membrane (Molecular Weight Cut Off 6000-8000 Spectrum, Netherlands), distilled water (Lion Waters Limited, Nsukka, Nigeria), sodium hydroxide, hydrochloric acid (BDH, England), commercial piroxicam gel (Roxy® Gel) (Bond Pharm. Nig. Ltd., Lagos, Nigeria). *Capra hircus* was obtained from a batch processed in Pharmaceutics Laboratory, University of Nigeria, Nsukka, Nigeria.

2.2. Tailor-made lipid matrix formulation.

The tailor-made lipid matrix was formulated by fusion method in water-bath using a hot plate (Ika RCT basic, Ika, Staufen, Germany), employing homolipid from CH and Transcutol®-HP in the ratio 2:1, which was optimized from our preliminary studies. Briefly, specified amounts of these lipids were weighed and melted together in temperature-regulated water bath at 70 ºC. The lipid melt was stirred until a homogenous admixture was obtained. This thereafter stirred at room temperature to get a solid mass. The lipid matrix was then properly stored until used.

2.3. Thermal characterization.

Thermal properties of pure piroxicam, Transcutol® HP, CH, and optimized lipid-matrix were assessed using 5 mg of each sample. First, empty aluminum pan were used to ascertain the baselines. Thereafter, weighed samples were sealed hermetically and a differential scanning calorimeter (DSC Q100 TA Instrument, Germany) was used to determine the thermal behaviours of the samples when heated between 20 – 250 °C at a heating rate of 5 °C/min, held at 80 °C for 10 min and cooled at 5 °C/min. Importantly, all the thermograms obtained were baseline-corrected.

The DSC analysis was extended to the solid lipid microparticles and gel formulations (representative batches).

2.4. Formulation of solid lipid microparticles (SLMs).

The SLMs were prepared by the melt-emulsification technique [42]. Briefly, the lipid matrix (15 g) was melted over a water bath in a thermo-controlled hot plate which was set at 80ºC. Solutol® HS-15 and Tween® 80 were added to the lipid matrix to enhance drug dissolution. Distilled water was added to Lutrol® F-68 and the temperature of the aqueous phase obtained was made uniform with that of the lipid matrix. The aqueous phase was poured into the lipid phase, and the Ultra-Turrax homogenizer (T-25 digital Ultra-Turrax; IKA, Staufen, Germany) was used to homogenize the two phases at 10,000 rpm for 5 min. Thereafter, the hot O/W emulsion obtained was collected in pre-warmed packages. These unloaded (zero-drug) SLMs were to serve as a control. By adding piroxicam (0.2, 0.5, and 1.0 %w/w) to the lipid matrix and following the above procedure, drug-loaded formulations were produced into three batches. The formulation composition is presented in Table 1.

Table 1. Formulation composition of the surface-engineered solid lipid microparticles.

Compositions	**Batch A (% quantity)**	**Batch B (% quantity)**	**Batch C (% quantities)**	**Batch D (% quantity)**
Piroxicam	0	0.2	0.5	1.0
Capra hircus (goat fat)	10	10	10	10
Transcutol® HP	5	5	5	5
Solutol®	3	3	3	3
Tween® 80	1	1	1	1
Lutrol® F68	2	2	2	2
Distilled water (q.s.) (ml)	79	78.8	78.5	78

2.5. Characterization of SLM.

2.5.1. Encapsulation efficiency (EE%) determination.

This was done by centrifuging a 6ml sample of piroxicam-loaded SLMs in a micro concentrator (Vivascience, Germany) at 3000 rpm for 120 min. After adequate dilution of the resultant supernatants with simulated intestinal fluid (SIF), the amount of un-encapsulated drug in the microparticles was analyzed by UV spectrophotometer (Unico 2102, England) at a predetermined wavelength of 345 nm. The EE% was calculated using equation (1) [1].

$$EE\ (\%) = \frac{Actual\ drug\ content}{Theoretical\ drug\ content} \times 100 \quad (1)$$

2.5.2. Determination of mean particle size.

The mean particle sizes of the SLMs were determined by polarized light microscopy (PLM). Briefly, a drop of an aqueous dispersion of each batch of the SLMs was introduced on a slide. This was covered with a cover slip and the image captured at X400 magnification. Average sizes of the particles were taken.

2.5.3. Short-term stability studies.

The formulated SLMs were left undisturbed at room temperature for 7 days and observed for physical examinations (phase separation and color/odor changes). In addition, the pH of the SLM formulations was periodically determined (on day-1, day-7, and day-30) by inserting the electrode of the potentiometer into each batch of the SLMs and recording the pH values. These short-term stability studies were carried out to determine the most stable (optimized) batch for further studies.

Furthermore, the short-term stability study was extended to the gel formulations.

2.6. Preparation of microgels.

The gels were prepared by the cold-dispersion method [65]. Two types of gelling agents were employed – poloxamer-based polymer: Poloxamer® 407 (P407) and polyacrylic acid-based polymer: Carbopol® 974 (C974P). Briefly, P407 was properly solubilized in distilled water followed by addition of propylene glycol, this was mixed until a homogenous semi-solid mass (hydrogel) was formed. The SLM formulations (1 ml) were added to the hydrogels and mixed thoroughly until homogenous semi-solid microgels were formed. Several batches of P407-based and C974P-based gel formulations were prepared, including plain hydrogel and plain and drug-loaded microgels. The C974P hydrogel/microgel was further neutralized with triethanolamine, and pH was adjusted to 5.5. All formulations were properly stored until used.

2.7. Characterization of the microgels.

2.7.1. Drug content determination.

A 2 g quantity of each gel preparation was weighed and placed in a 100-ml volumetric flask. Then, 10 ml of methanol was added, mixed thoroughly, and stirred continuously for 30 min. The volume was made up to the mark with the solvent, then centrifuged at 4000 rpm for 30 min. and filtered. The content of piroxicam in the solution was spectrophotometrically assayed at 345 nm, and the drug content efficiency was determined employing equation (2).

$$Drug\ content\ efficiecy\ (\%) = \frac{Actual\ drug\ content}{Theoretical\ drug\ content}\ X\ 100 \qquad (2)$$

2.7.2. Spreadability determination.

This study was carried out by adopting a reported technique [65]. Briefly, 0.5 g of each test sample was placed in-between two unmarked upper and marked lower glass slides after which varying weights (50, 100, 200, and 300 g) were placed on the upper slide and respective diameters occupied by the spreading gel were employed to ascertain the area of spread (length x width). The experiment was replicated using the same weight in each case [65].

2.7.3. Rheological assessment.

The viscosity assessment of all formulations was done using NDJ-55 digital viscometer. The spindle at a speed of 12 rpm was inserted into 10 g of the gel for 1min. The viscosity was read off the display and recorded.

2.7.4. *In-vitro* drug release studies.

Release study was carried out using a dialysis bag placed in the release medium (phosphate buffer, pH 5.5 for topical microgels, and pH 7.4 for oral SLMs) under constant hot plate magnetic stirring [42,59]. The dialysis membrane (Molecular Weight Cut Off 6000-8000 Spectrum, Netherlands) was soaked for 24 h after which one end of the membrane was tied, and 5 ml of each batch of the drug-loaded formulations (SLMs and microgels) was introduced into the membrane. The loose end was tied afterward and suspended in 200 ml of the medium, all in a thermostatic rotating basket dissolution sytem. Samples were collected at various time intervals (0.5, 1, 2, 4, 6, 8, 10, and 12 h) and replaced with equal volume of phosphate buffer

serving as the dissolution medium (to maintain sink condition). The samples obtained were analyzed with a UV-vis spectrophotometer at a predetermined wavelength of 375 nm. The concentration of piroxicam present in the samples was calculated and recorded. This entire procedure was repeated for pure piroxicam samples and commercial samples (Roxy® Gel), which served as controls for the SLMs and microgels, respectively.

2.7.5. Anti-inflammatory investigation.

The anti–inflammatory activity of the formulations (piroxicam-loaded oral SLMs and topical microgels) was carried out using the rat paw edema test [44,71]. The guidelins of the Animal Ethics Committee of the Faculty of Pharmaceutical Sciences, University of Nigeria, Nsukka were followed and fresh undiluted egg albumin served as the phlogistic agent [50]. Forty-eight male and female adult Wistar rats (120 – 200 g) were acclimatized for 10 days, fasted and deprived of water for 12 (to ensure uniform hydration and to minimize variability in oedematous response) after which they were divided into eight groups of six rats per group as follows:

Group-1 represents animals that received unloaded SLM (negative control for SLMs).
Group-2 represents animals that received pure piroxicam drug (reference or positive control for SLMs).
Group-3 represents animals that received optimized SLM (batch B).
Group-4 represents animals that received optimized poloxamer-based microgels.
Group-5 represents animals that received optimized Carbopol-based microgels.
Group-6 represents the animal that received unloaded poloxamer-based microgels (negative control for P408 microgels).
Group-7 represents animals that received unloaded Carbopol based microgels (negative control for C974P microgels).
Group-8 represents animals that received a commercial sample of piroxicam gel (Roxy® Gel) (reference or positive control for microgels).

Rats in groups 1-3 were used to determine the anti-inflammatory activity of the optimized SLM formulation (batch B) and a pure sample of piroxicam in the following order: Negative control (group-1) received 10 mg/kg of unloaded SLMs, Positive control (group-2) received 10 mg/kg of a pure sample of piroxicam while optimized piroxicam–loaded SLMs (batch B) equivalent to 10 mg/kg body weight was given per oral to the animals in group-3. Thirty minutes post-treatment, edema was induced by injection of 0.1 ml fresh undiluted egg–albumin into the subplantar region of the right hind paw of the rats [1,2]. Rats in groups 4-8 were used in determining the anti-inflammatory effect of the microgels and commercial sample in the following order: one gram of optimized piroxicam loaded, poloxamer-based microgel (containing 0.37 mg piroxicam) was applied to the sub plantar surface of the hind Paw of rats in group-4 by gentle rubbing 50 times with the index finger [63]. One gram of optimized piroxicam-loaded Carbopol-based microgel was applied to rats in group-5 using the same procedure. Rats in group-6 and group-7 served as negative controls and received 1 g of unloaded poloxamer-based and Carbopol-based microgels (hydrogels), respectively. Rats in group-8 received 74 mg of commercial piroxicam gel (Roxy® Gel) containing 0.37 mg piroxicam, which is equivalent to 1 g of microgel formulations. Induction of edema was done at 0.5 hour after treatment by administering the phlogistic agent on the right had paw of the animals [50]. Plethysmometer was then used to determine the amount of distilled water

displaced by the treated right hind paw of the animals before and at 0.5, 1, 2, 3, 4, 5, and 6 h post-edema induction. The percent inhibition of edema was calculated using equation (3) [71].

$$\%\ Inhibition\ of\ oedema = 1 - \left[\frac{a-x}{b-y}\right] \times 100 \quad (3)$$

Where 'a' is the mean paw volume of treated rats after egg albumin injection, 'x' is the mean paw volume of treated rats before egg albumin injection, 'b' is the mean paw volume of control rats after egg albumin injection, and 'y' is the mean paw volume of control rats before egg albumin injection.

2.8. Statistical analysis.

Data obtained from the study were analyzed statistically using one-way analysis of variance (ANOVA), and considered statistically significant at $p < 0.05$.

3. Results and Discussion

3.1. Thermal properties of tailor-made lipid matrix.

The DSC thermograms of the individual lipids and optimized tailor-made lipid matrix are shown in Figure 1. Homolipids from *Capra hircus* (goat fat) had a melting peak of 53.7 °C and an enthalpy of -16.42 mW/mg (Figure 1A). Transcutol®-HP alone had a melting temperature of 174.1 °C and an enthalpy of -24.35 mW/mg (Figure 1B). When Transcutol® HP was incorporated into the *Capra hircus* to form the tailor-made lipid matrix, the thermal properties changed to two melting peaks of 53.4 and 100.8 °C, with corresponding enthalpies of -31.63 and - 11.42 mW/mg, respectively (Figure 1C).

The thermal analysis shows that the CH-Transcutol® HP lipid matrix melted with endothermic decomposition. The increase in melting peak in one of the modifications suggests that the physical mixture of CH and Transcutol®-HP was more stable than the individual components alone. The results showed that structuring of CH with Transcutol®-HP produced a tailor-made matrix with low enthalpy. Generally, a decrease in enthalpy implies reduction in crystallinity of lipid matrices [46]. Therefore, the CH-Transcutol® HP lipid matrix generated an disordered matrix (attributed to disorganization of crystals of individual lipids following melting and subsequent solidification), which ultimately would enhance drug encapsulation [46]. The interaction of different fatty acid contents of the lipids might be responsible for the crystal disorganization and rearrangement of the individual lipids [45]. By implication, the reduction in enthalpy shows that CH/Transcutol®-HP admixture was less crystalline and hence has a tendency to entrap more drugs.

3.2 Physicochemical properties of the SLMs.

3.2.1 Encapsulation efficiency.

Table 2 depicts the results of the loading efficiency of the SLMs. It can be seen that the encapsulation efficiency of the SLMs loaded with 0.2 % piroxicam was higher than the lipid matrix loaded with 0.5 and 1.0 % of the drug. In other words, SLM batch B had the highest encapsulation efficiency (89.16 ± 0.4 %), followed closely by SLM batch D with EE% of 79.55 ± 0.3 %, and SLM batch C with EE% of 59.96 ± 0.2 %.

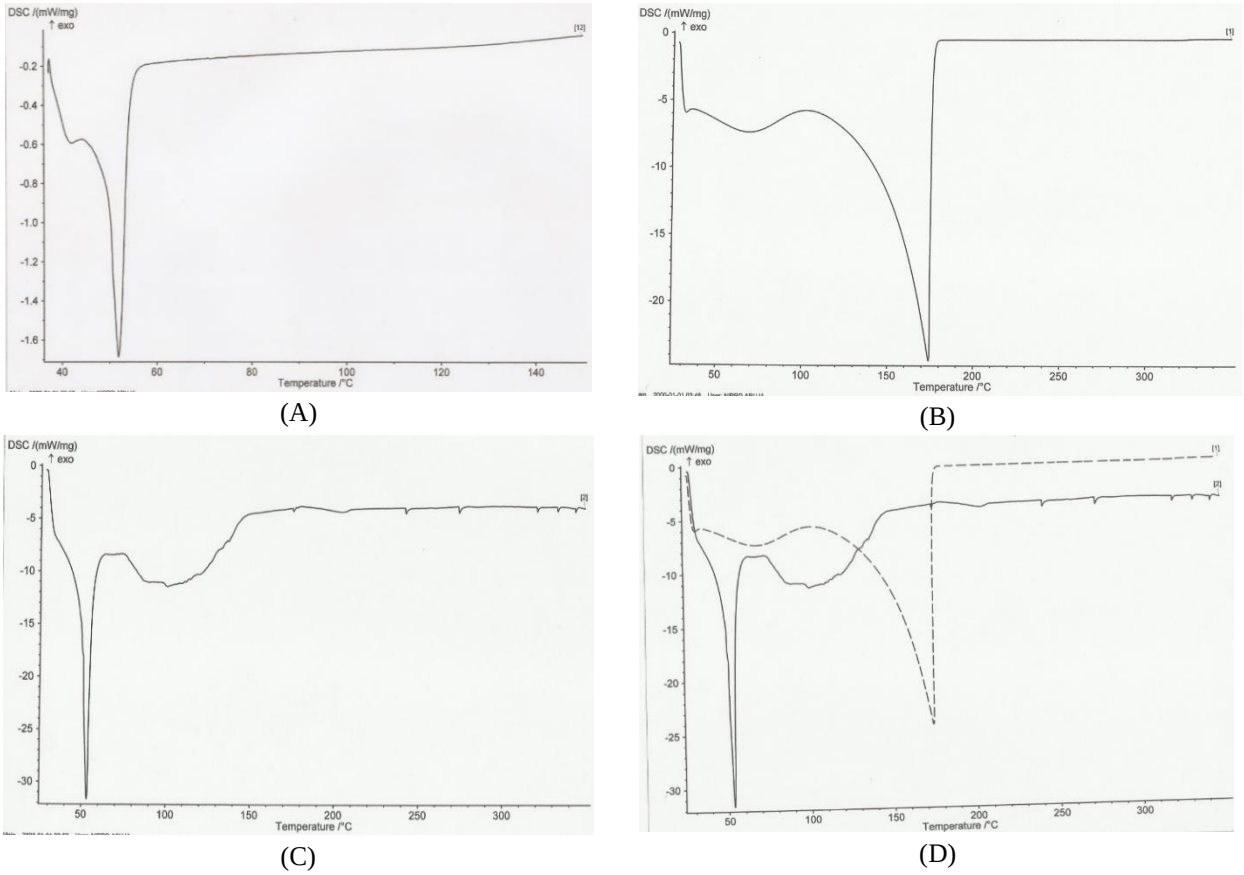

Figure 1. Differential scanning calorimetry (DSC) thermograms of *Capra hircus*, CH (goat fat) (A), Transcutol® HP (B), *Capra hircus*/Transcutol® HP admixture (lipid matrix) (C), Transcutol® HP and lipid matrix in superposition (D). **Key**: For superimposed figures (D), 1 represents Transcutol® HP while 2 represents the tailor-made *Capra hircus*/Transcutol® HP lipid matrix.

A good number of NSAIDs with various degrees of lipophilicity have been incorporated into SLMs [1-3,50]. The EE% is an important tool to evaluate a potential drug carrier system and for SLMs, it is obviously desirable to produce microparticles with high drug content in order to decrease the number of microparticles to be administered. For this purpose, a sufficiently high solubility of the drug in the lipid melt would facilitate loading capacity. Various factors affect the loading efficiency of the drug in the lipid, including lipid material polymorphicity, drug solubility in the melted lipid, structure of the lipid matrix, and miscibility of the lipid melt and drug melt [72]. It was observed that the amount of drug loaded in the SLMs affected the encapsulation efficiency. However, all the batches showed high encapsulation efficiency, which may be due to the lipophilicity of piroxicam. The highest drug loading capacity obtained with the optimized SLM means that, on the one hand, the matrix had enormous spaces which accommodated the piroxicam, and on the other hand, the solubilizers promoted drug solubilization. The high loading efficiency also agrees with the observation from solid-state characterization using DSC, where the tailor-made lipid matrix showed an imperfect and disordered matrix with numerous spaces for drug loading, which is consistent with earlier studies [1-3,50].

Table 2. Some physicochemical properties of solid lipid microparticles and microgels formulated with tailor-made *Capra hircus*/Transcutol® HP composite.

Composition (g)	**Particle size (µm ± SEM)[a]**	**Drug content or encapsulation (% ± SEM)[b]**	**pH[b,c]**	
			Day-1	**Day-7** **Day-30**
Zero drug SLM-A	1.704±0.02	-	4.2±0.1	4.1±0.3 4.0±0.1

Composition (g)	Particle size (µm ± SEM)[a]	Drug content or encapsulation (% ± SEM)[b]	pH[b,c]		
			Day-1	Day-7	Day-30
Drug-loaded SLM-B	2.338±0.05	89.16±0.4	4.4±0.2	4.3±0.1	4.3±0.2
Drug-loaded SLM-C	1.410±0.02	59.96±0.2	4.4±0.1	4.4±0.2	4.3±0.3
Drug-loaded SLM-D	1.057±0.01	79.55±0.3	4.6±0.3	4.5±0.3	4.5±0.2
C974-based unloaded microgel	1.234±0.03	-	5.6±0.4	5.5±0.4	5.4±0.3
C974-based batch B microgel	1.880±0.04	77.24±0.9	5.5±0.3	5.6±0.2	5.6±0.4
C974-based batch C microgel	1.410±0.02	80.76±1.2	5.5±0.1	5.4±0.1	5.4±0.1
C974-based batch D microgel	1.939±0.01	75.62±0.8	5.7±0.2	5.6±0.3	5.5±0.4
C974-based hydrogel	-	-	5.5±0.3	5.4±0.2	5.4±0.3
P407-based unloaded microgel	2.115±0.04	-	5.5±0.1	5.6±0.4	5.6±0.4
P407-based batch B microgel	1.763±0.02	94.05±1.4	5.4±0.2	5.5±0.3	5.5±0.1
P407-based batch C microgel	2.028±0.01	86.02±0.9	5.5±0.1	5.6±0.3	5.6±0.2
P407-based batch D microgel	2.038±0.03	85.19±0.6	5.6±0.3	5.5±0.1	5.4±0.3
P407-based hydrogel	-	-	5.4±0.2	5.4±0.2	5.3±0.1

Key: [a]n = 5, [b]n = 3, [c]Mean ± SEM, SEM is the standard error of mean; zero drugs SLM-A means solid lipid microparticles formulated without piroxicam; drug-loaded SLM-B, drug-loaded SLM C and drug-loaded SLM-D are solid lipid microparticles containing 0.2, 0.5 and 1.0 %w/w of piroxicam, respectively, in the formulations. P407 means Poloxamer® 407; C974 means Carbopol® 974P; P407-based batch B microgel, P407-based batch C microgel, and P407-based batch D microgel are poloxamer-based microgels containing 0.2, 0.5 and 1.0 %w/w of piroxicam, respectively, in the solid lipid microparticles used in formulating the drug-loaded poloxamer-based microgels; C974-based batch B microgel, C974-based batch C microgel and C974-based batch D microgel are Carbopol-based microgels containing 0.2, 0.5 and 1.0 %w/w of piroxicam, respectively, in the solid lipid microparticles used in formulating the drug-loaded Carbopol-based microgels; C974-based unloaded microgel and P407-based unloaded microgel are microgels formulated with zero drug SLM-A and based on Carbopol® 974P and Poloxamer® 407, respectively; while C974-based hydrogel and P407-based hydrogel are plain hydrogels prepared with Carbopol® 974P and Poloxamer® 407, respectively.

3.2.2. Mean particle size and morphology.

Table 2 shows the mean particle sizes of all batches of the SLMs, which were in the sub-micron range. The mean particle size of unloaded SLMs (batch A) was 1.704 ± 0.02 µm while the mean particle sizes of piroxicam-loaded SLMs were in the range of 1.057 ± 0.01 to 2.338 ± 0.05 µm, with SLM batches D and B having the least and highest mean particle sizes, respectively. The mean particle sizes of SLMs containing piroxicam and the zero-drug SLMs did not show any significant difference ($p > 0.05$). The photomicrographs of the SLMs are depicted in Figure 2. It could be seen that they comprise of spherical and non-spherical particles.

The mean particle size range obtained with the SLMs formulations is within the micro-meter-sized particles reported in the literature for piroxicam microparticles [1-3], which would exhibit greatly increased surface area leading to enhanced permeability across biological membranes. The ratio of drug to lipid affected the size of the SLMs produced. Increase in the concentration of the loaded drug decreased the particle size of the SLMs, which is in contrast with the work done by Joseph and co-researchers [73], who prepared piroxicam-loaded polycarbonate microspheres. However, the particle sizes of SLMs formulations could be affected by several factors, including pharmaceutical excipients, particle size growth, particle

crystalline habit, homogenization pressure and degree, etc [74]. The morphological features of the SLMs are indicative of physical stability due to absence of particle agglomeration[74].

3.2.3. Physical examination and pH analysis.

Upon physical examination of the SLM formulations, it was observed that batch B SLM was very stable and did not separate on standing for 30 days. In addition, the short-term pH-dependent time-resolved stability tests on the SLMs showed insignificant deviation ($p > 0.05$) in the pH values, as shown in Table 2. However, drug-loaded SLMs had higher pH values than unloaded SLM. In addition, there was a concentration-dependent increase in pH of drug-loaded SLMs (Table 2). Overall, Table 2 showed that the pH values of the SLMs varied from between 4.2 ± 0.1 to 4.6 ± 0.3 within 24 h of preparation to between 4.0 ± 0.1 and 4.5 ± 0.2 within 1 month of preparation.

The pH analysis performed in this study was essential for pharmaceutical formulations because wide variations in pH can irritate biological membranes. However, for the SLMs developed in this study, there were insignificant variations in the pH values following short-term stability studies, and the pH range of the SLMs falls within the acceptable pH range for oral formulations.

Based on the fact that SLM batch B gave the best results concerning physicochemical and short-term stability studies, it was selected as the optimized batch for further investigations. With larger sub-micron particle size due to increased drug entrapment, batch B SLM would be expected to have higher edema inhibition.

3.2.4. Thermodynamic stability of piroxicam in the SLMs.

Figure 3 shows the DSC thermographs of plain solid lipid microparticles, piroxicam, and drug-loaded formulation in superposition. The DSC thermograph of pure piroxicam exhibited a major sharp endothermic single peak indicating melting at 203.1 °C and enthalpy of -29 mW/mg as presented in Figure 3(A). The unloaded SLMs show a melting peak of 121.6 °C and an enthalpy of -193 mW/mg (Figure 3B). Optimized piroxicam-loaded SLMs batch B had a melting peak of 118.1 °C and an enthalpy of -167 mW/mg (Figure 3C). It could be seen that drug-loaded formulation gave lower melting point and enthalpy than pure piroxicam as the melting temperature was lowered from 121.6 °C to 118.1 °C and the enthalpy from -193 mW/mg to -167 mW/mg.

Overall, the DSC thermograms of the drug showed a sharp endothermic peak which revealed high crystallinity and purity consistent with earlier report [1]. Total disappearance of the drug peak was observed in the SLM formulations containing piroxicam such that it became indistinguishable from the zero-drug-loaded formulations. Even though this does not guarantee the complete absence of drug crystals yet it suggests that there was an improved dissolution of the drug in the matrices. It has been observed that polymorphic transformations occur during preparation and storage [1,53]. Since a decrease in the enthalpy correlates with enhanced drug entrapment in the matrix core, this agrees with the good encapsulation efficiency (89.16 ± 0.4 %) obtained with the optimized SLM batch B.

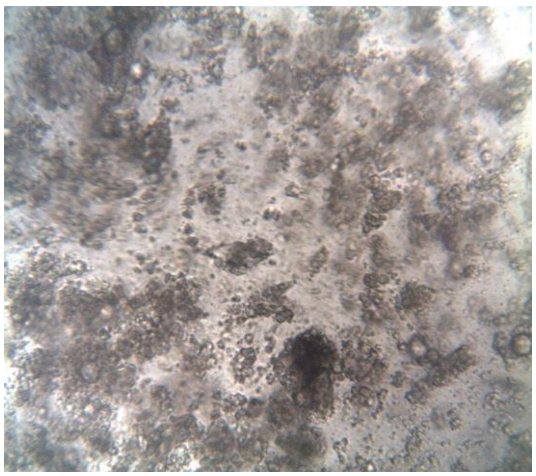

(A)

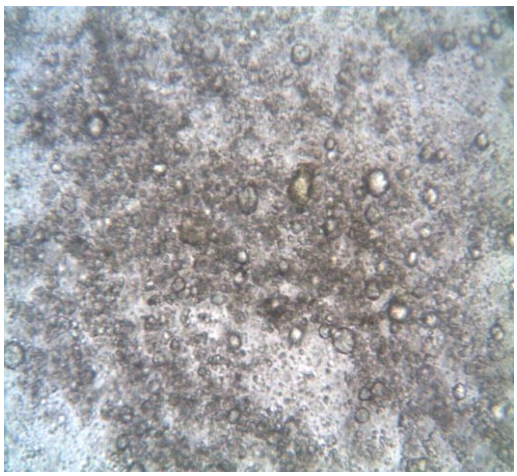

(B)

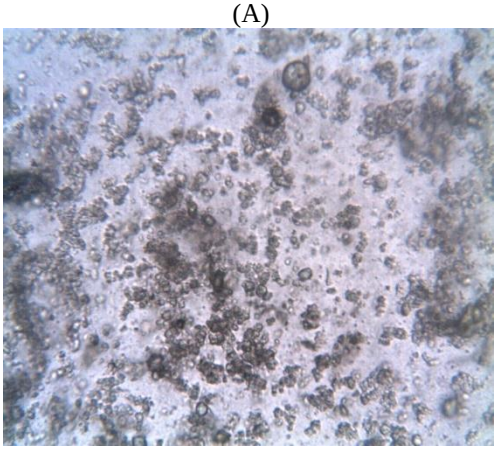

(C)

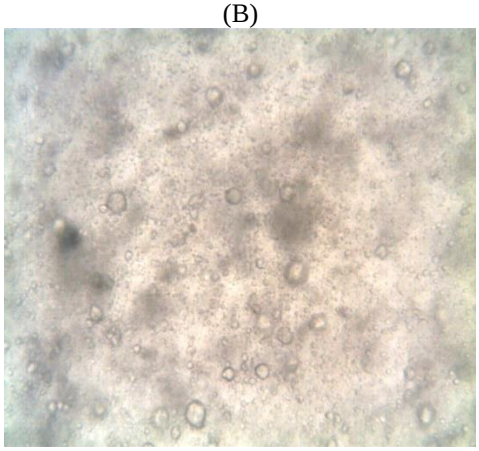

(D)

Figure 2. Photomicrographs of the SLMs formulations. A-D represents batches A to D SLMs.

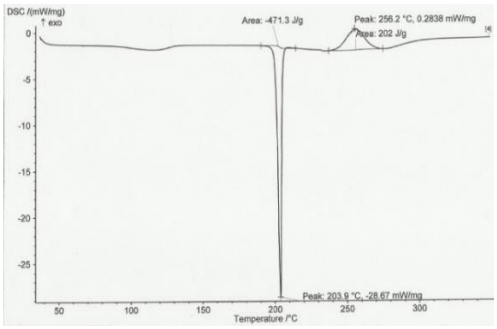

(A)

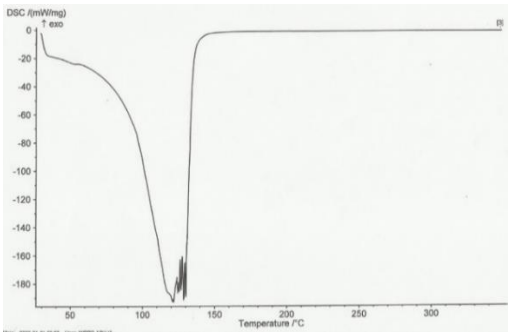

(B)

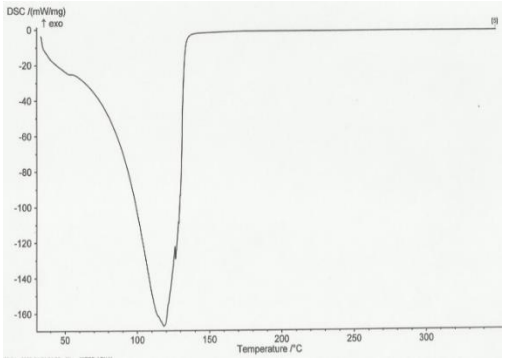

(C)

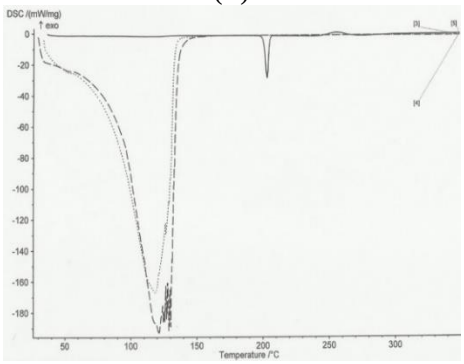

(D)

Figure 3. Differential scanning calorimetry (DSC) thermograms of piroxicam (A), unloaded SLMs formulation (B), piroxicam-loaded SLMs formulation (C), SLMs formulations in superposition (D).

Key: For superimposed figures (D), 3 represents unloaded SLM formulation, 4 represents pure piroxicam sample while 5 is piroxicam-loaded SLMs (optimized SLM formulation).

3.3. Physicochemical properties of the gel formulations.

3.3.1. Organoleptic and pH analyses.

The gel formulations were consistent, odorless, and had uniform color. Results of the pH studies (Table 2) showed that, for Carbopol-based gel formulations, the pH of plain C974 hydrogel varied from 5.5 ± 0.3 within 24 h of preparation to 5.4 ± 0.3 within 1 month of preparation, the pH of unloaded C974 microgel varied from 5.6 ± 0.4 within 24 h of preparation to 5.4 ± 0.3 within 1 month of preparation, whereas the pH of piroxicam-loaded C974 microgel varied from between 5.5 ± 0.1 to 5.7 ± 0.2 within 24 h of preparation to between 5.4 ± 0.1 and 5.6 ± 0.4 within 1 month of preparation. Similarly, for poloxamer-based gel formulations, the pH of plain P407 hydrogel varied from 5.4 ± 0.2 within 24 h of preparation to 5.3 ± 0.1 within 1 month of preparation, the pH of unloaded P407 microgel varied from 5.5 ± 0.1 within 24 h of preparation to 5.6 ± 0.4 within 1 month of preparation, whereas the pH of piroxicam-loaded P407 microgel varied from between 5.4 ± 0.2 to 5.6 ± 0.3 within 24 h of preparation to between 5.3 ± 0.1 and 5.6 ± 0.2 within 1 month of preparation.

Overall, the pH values of the gel formulations, which generally did not deviate from the reported pH range of the skin (range = 4.5–6.5) [65-68], indicated the suitability of the developed gel formulations for topical delivery of piroxicam, consistent with previous reports on topical delivery of bioactive agents [34]. Thus, the optimized formulations are safe for use on the skin.

3.3.2. Drug content of the microgels.

Table 2 shows the percentage drug content of the mucoadhesive gel formulations. Carbopol-based microgels showed percentage drug content in the range of 75.62 ± 0.8 to 80.76 ± 1.2 %, whereas poloxamer-based microgels had percentage drug content in the range of 85.19 ± 0.6 to 94.05 ± 1.4. Results showed that poloxamer-based microgels had higher percentage drug content that Carbopol-based microgels, with poloxamer-based microgels containing 0.2 %w/w of piroxicam (lowest drug loading) in the solid lipid microparticles used in formulating the drug-loaded poloxamer-based microgels having the highest whereas Carbopol-based microgels containing 1.0 %w/w of piroxicam (greatest drug loading) in the solid lipid microparticles used in formulating the drug-loaded Carbopol-based microgels having the least.

The microgel formulations had good percent drug content. Microgel drug content analysis agrees that independent of the drug being incorporated or attached, it is still possible to achieve high drug content whenever the drug-lipid interaction favors attachment/incorporation [73]. Therefore, to improve skin uptake and targeting, a semi-solid vehicle, as has been demonstrated in this study, remains a standard approach that exhibits high stability and low toxicity.

3.3.3. Mean particle size and morphology.

Table 2 shows the mean particle size of the microgels, while the micrographs of the gel formulations are depicted in Figure 4. It could be deciphered that Carbopol-based microgels had smaller mean particle sizes than poloxamer-based microgels. For Carbopol-based microgels, the mean particle size of unloaded C974-based microgel was 1.234 ± 0.03 µm while the mean particle sizes of piroxicam-loaded C974-based microgels were in the range of 1.410 ± 0.02 to 1.939 ± 0.01 µm, with batch D containing 1.0 %w/w of piroxicam (greatest drug

loading) in the solid lipid microparticles used in formulating the drug-loaded Carbopol-based microgels having the largest mean particle sizes. For poloxamer-based microgels, the mean particle size of unloaded P407-based microgel was 2.11 ± 0.04 µm while the mean particle sizes of piroxicam-loaded P407-based microgels were in the range of 1.763 ± 0.02 to 2.038 ± 0.03 µm, with batch B containing 0.2 %w/w of piroxicam (lowest drug loading) in the solid lipid microparticles used in formulating the drug-loaded poloxamer-based microgels having the least mean particle sizes. Moreover, the microgels showed the microstructures of the gel as well as the dispersed lipidic particles.

The particle sizes of the microgel formulations were generally small. By implication, this shows the suitability of the developed microgels for topical skin delivery of piroxicam, consistent with previous reports [34]. Decrease in the particle size would facilitate penetration of the particulate formulations to the skin layers [65].

3.3.4. Spreadability.

Figure 5 depicts the spreadability of the gel formulations. It could be seen from the figure that poloxamer-based microgels were more spreadable than Carbopol-based microgels. Among Carbopol-based gel formulations (Figure 5A), the plain hydrogel was the most spreadable, whereas among poloxamer-based gel formulations (Figure 5B), unloaded microgel had the highest spreadability, followed by the plain hydrogel and lastly, the drug-loaded microgel formulations. Moreover, there was a load-dependent increase in the area of spread across all batches of the gel formulations.

The higher spreadability of poloxamer-based microgels vis-à-vis Carbopol-based microgels, consistent with earlier reports on topical microgels [65,68], would enhance the drug administration, release and anti-inflammatory activity of piroxicam. Meanwhile, C974P NF polymer is a highly cross-linked polymer and it has been used to produce highly viscous gels with rheology similar to mayonnaise (low spreadability) [65].

3.3.5. Rheological determination.

The results of the rheological evaluation are shown in Figure 6. Incorporation of SLMs into the Carbopol-based hydrogel caused a reduction in viscosity across all batches of Carbopol-based microgels, while the incorporation of SLMs into poloxamer-based hydrogel slightly increased viscosity across all batches of poloxamer-based microgels. However, all drug-loaded C974-based microgels were more viscous than all batches of drug-loaded P407-based microgels. Moreover, decreased viscosity was generally observed at high concentrations of the microgels.

The highly viscous nature of C974-based microgels vis-à-vis P407-based microgels would lower the spreadibility Carbopol-based microgel, which invariably would result in lower pharmacodynamic activity vis-à-vis the poloxamer-based microgel. This is in consonance with earlier reports on microgels [65,68].

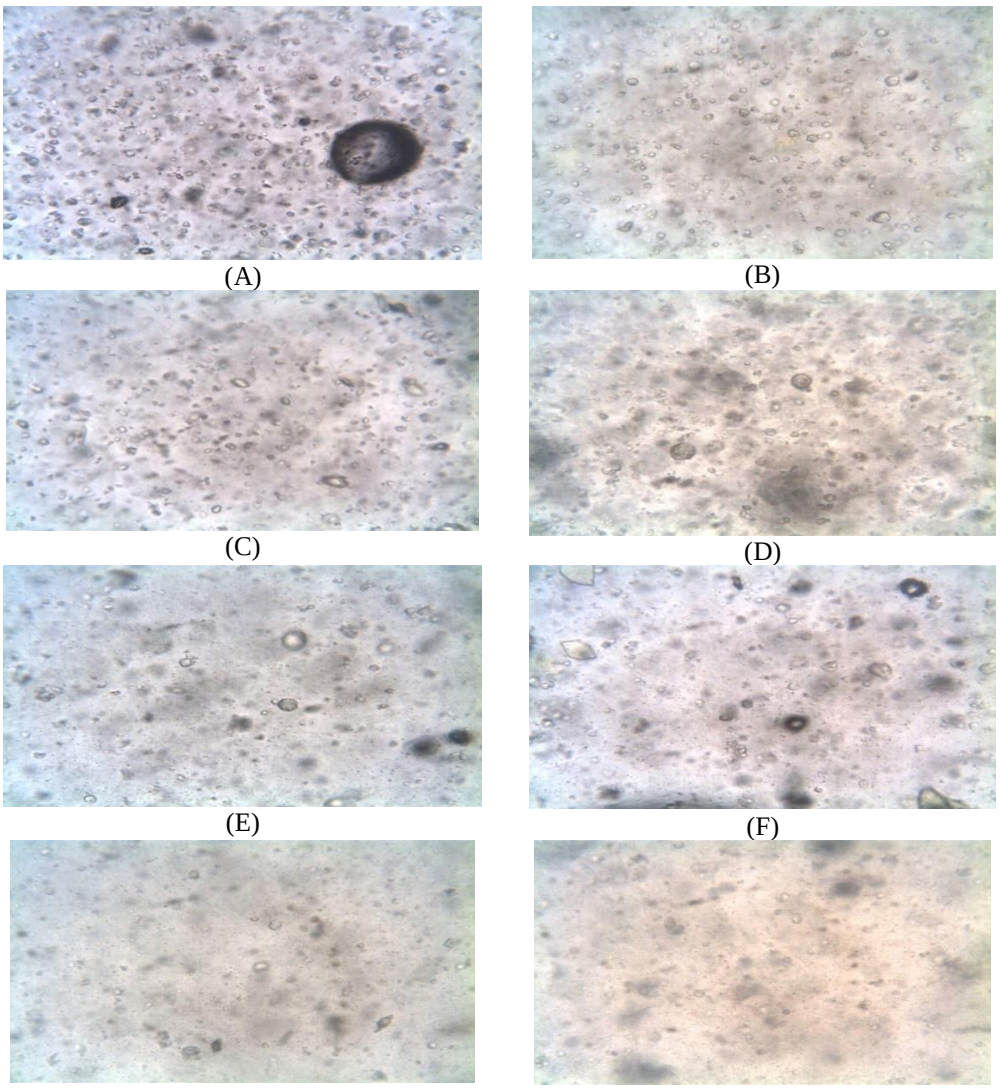

(A) (B) (C) (D) (E) (F) (G) (H)

Figure 4. Photomicrographs of the microgels formulations.

Keys: A-D represents Carbopol-based microgels batches A to D while E-H represents poloxamer-based microgels batches A to D.

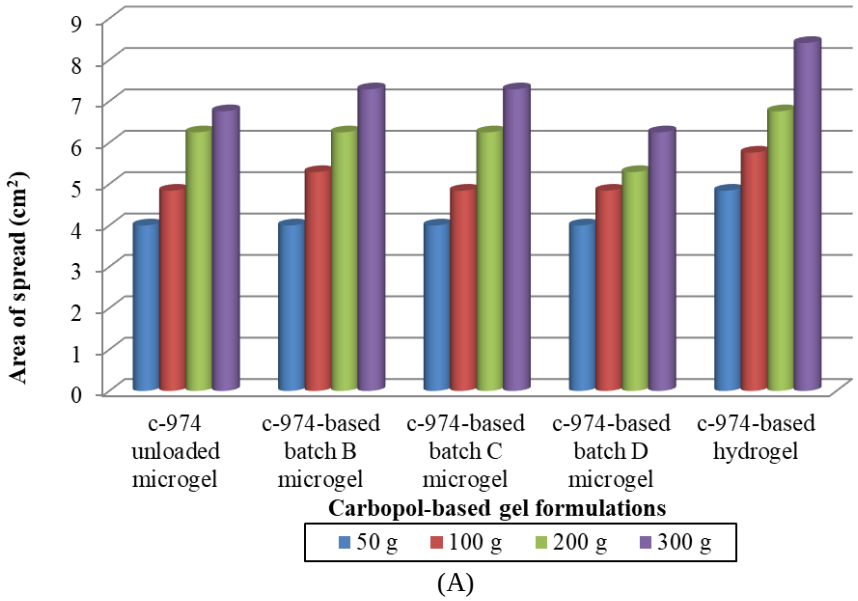

(A)

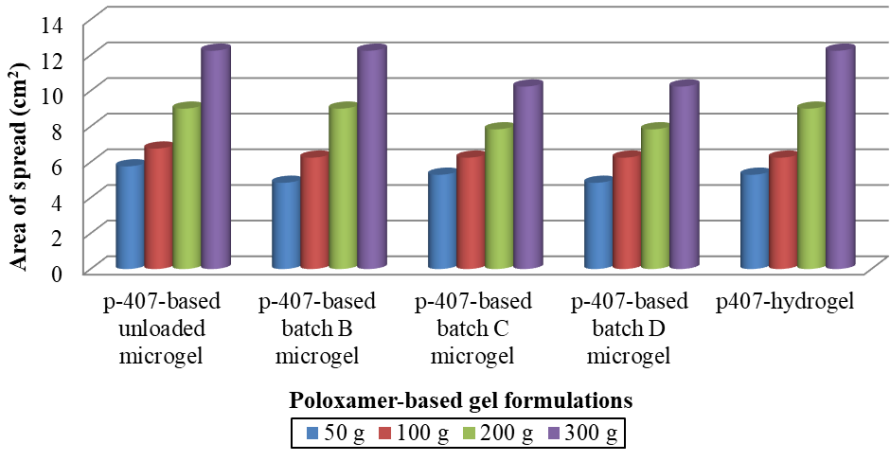

(B)

Figure 5. Spreadability of (A) Carbopol-based gel formulations and (B) Poloxamer-based gel formulations.

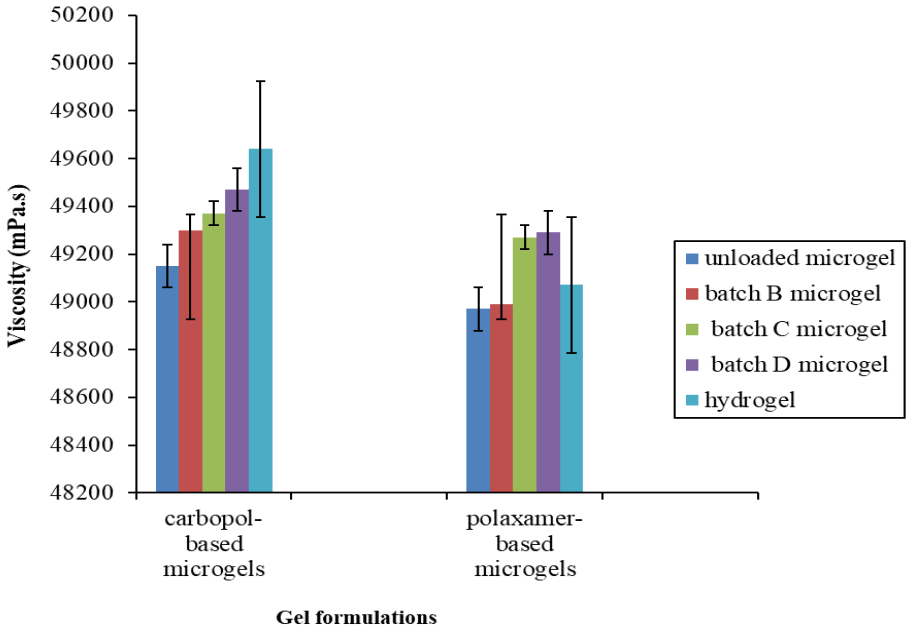

Figure 6. Viscosity profiles of the gel formulations.

3.3.6. Drug-excipient compatibility of the gel formulations.

The thermal properties of Carbopol plain hydrogel, Carbopol-based unloaded microgels, piroxicam-loaded Carbopol-based microgels, Carbopol-based formulations alongside pure piroxicam in superposition, poloxamer-based plain hydrogel, poloxamer-based unloaded microgels, piroxicam-loaded poloxamer-based microgels and poloxamer-based formulations alongside pure piroxicam in superposition are shown in Figures 7A- H, respectively. It can be deciphered from the figure that, correlating the thermal properties of the plain hydrogels, Carbopol-based hydrogel had a melting peak of 103.9 °C and an enthalpy of -70.05 mW/mg (Figure 7A) while poloxamer-based hydrogel exhibited a melting peak of 116.4 °C and a higher enthalpy of -139.4 mW/mg (Figure 7E). Furthermore, in correlation of the thermal properties of the microgels, the melting peaks of poloxamer-based unloaded microgels and Carbopol-based unloaded microgels were 134 and 119.1 °C, respectively, with corresponding enthalpies of -304.2 and -160.2 mW/mg (Figures 7B and 7F). Obviously, glass

transition (change in heat capacity without heat being absorbed or evolved.) was observed in the DSC trace of poloxamer-based unloaded microgels (Figure 7F). Clearly, there were modifications in melting point values and enthalpies for piroxicam-loaded microgels compared to the thermal properties of plain hydrogels, unloaded microgels, and the drug. The results showed that piroxicam-loaded Carbopol-based microgel showed a melting peak of 125.2 °C with the corresponding enthalpy of - 119.3 mW/mg (Figure 7C) while piroxicam-loaded poloxamer-based microgel showed melting peak of 105.7 °C with the corresponding enthalpy of - 103.9 mW/mg (Figure 7G).

Furthermore, there were modifications in melting point values and enthalpies for piroxicam-loaded microgels compared to the thermal properties of plain hydrogels, unloaded microgels, and the drug. Since higher melting point values implies greater crystallinity, [1-3], it follows that both Carbopol-based and poloxamer-based piroxicam-loaded microgels were less crystalline than piroxicam as the drug was molecularly dispersed in the microgels. Moreover, the physicochemical compatibility in the microgels of the drug, surface-engineered SLMs, and polymeric hydrogels of C974 and P407 studied by DSC suggested the absence of any incompatibility. The results showed that piroxicam, SLMs and hydrogel polymers (C974 and P407) are compatible as also indicates the stability of the drug in the drug-loaded microgels. This was because piroxicam-loaded microgels gave lower melting point values than the drug, implying that the drug existed in an amorphous state in the formulations, similar to recent reports [65,68,74].

3.3.7. *In-vitro* drug release from the SLMs and gel formulations.

The release profiles of piroxicam from the oral SLMs and topical microgels in corresponding phosphate buffers of pH 5.5 and 7.4 are shown in Figures 8A and 8B, respectively. The results indicate a very significant release of piroxicam from the SLMs as against a retarded release recorded with highly lipophilic pure piroxicam powder. It can be deduced from Figure 8A that, among piroxicam-loaded SLMs, the optimized batch B SLM with the greatest EE% released the highest amount of piroxicam (76.72 ± 0.9 %) after 12 h, whereas SLM batches C and D gave lower percentages of drug release (42.07 ± 0.3 and 45.75 ± 0.8 %, respectively). After 12 h, drug dissolution was higher in the drug-loaded microparticles than in the pure piroxicam sample (reference) (28.87 ± 0.9 %). Similarly, for topical microgels, Figure 8B shows that optimized poloxamer-based microgel, as well as marketed gel formulation, had higher percentages of drug release (90.2 ± 0.8 % and 81.74 ± 0.2 %, respectively) than Carbopol-based microgels (62.01 ± 0.5 %) during the 12 h period of study.

The drug release results correlated well with the result obtained from the drug loading efficiency. This might be responsible for the lower percentage release obtained with SLMs batch D compared with SLMs batch B. The surfactant properties of the excipients used in formulating the SLMs must have improved the aqueous solubility of poorly water-soluble piroxicam and hence the improved drug release into the medium (phosphate buffer). This is in line with previous studies where SLMs were employed to improve aqueous solubility and hence bioavailability of piroxicam [1-3]. The results of this study also agree with earlier studies that employed CH-based and Transcutol-based formulations for enhanced oral delivery of bioactive agents [41,57,58,70,71].

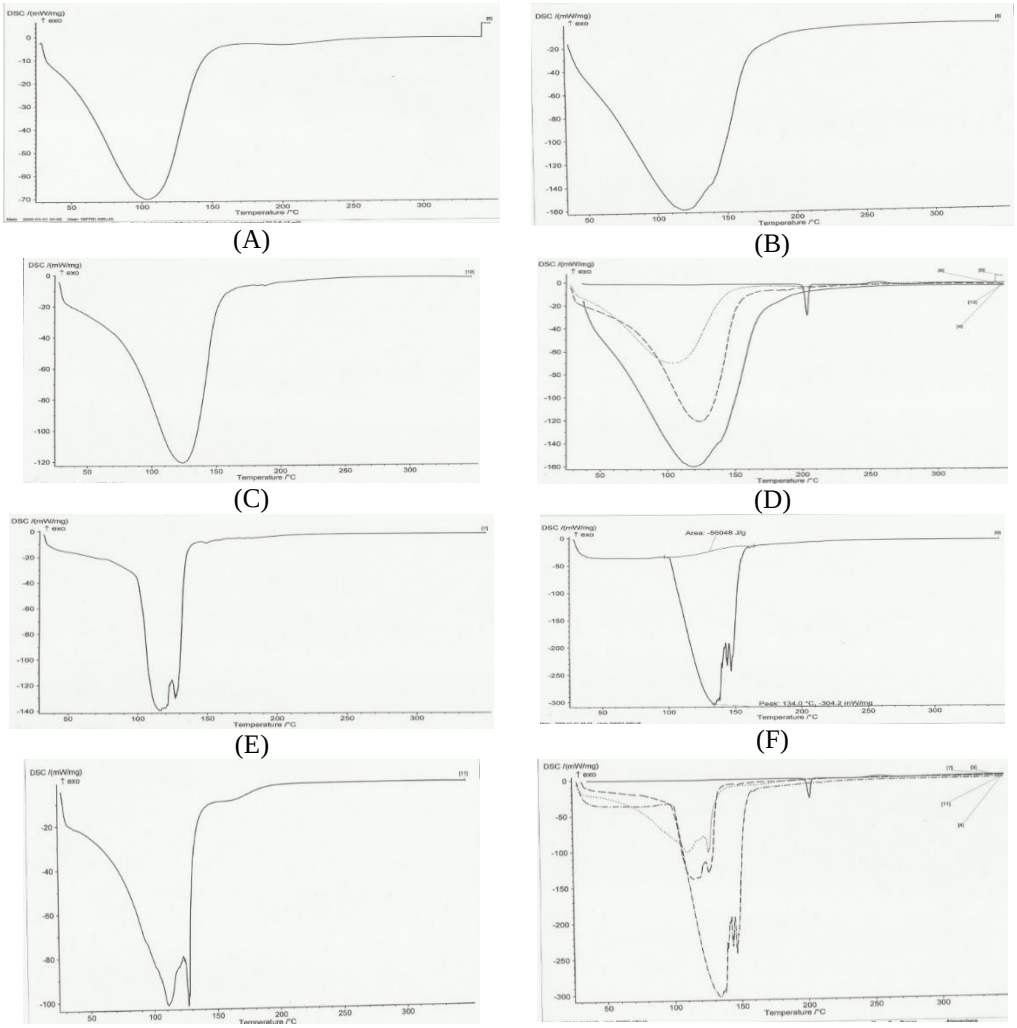

(A) (B) (C) (D) (E) (F) (G) (H)

Figure 7. Differential scanning calorimetry (DSC) thermograms of Carbopol plain hydrogel (A), Carbopol-based unloaded microgels (B), piroxicam-loaded Carbopol-based microgels (C), Carbopol-based formulations alongside pure piroxicam in superposition (D), Poloxamer-based plain hydrogel (E), Poloxamer-based unloaded microgels (F), piroxicam-loaded Poloxamer-based microgels (G), Poloxamer-based formulations alongside pure piroxicam in superposition (H). **Key**: For superimposed figures (D and H), 4 means pure piroxicam sample, 6 is Carbopol-based plain hydrogel, 7 is poloxamer-based plain hydrogel, 8 represents Carbopol-based unloaded microgel, 9 represents poloxamer-based unloaded microgel, 10 is piroxicam-loaded Carbopol-based microgel while 11 is piroxicam-loaded poloxamer-based microgel.

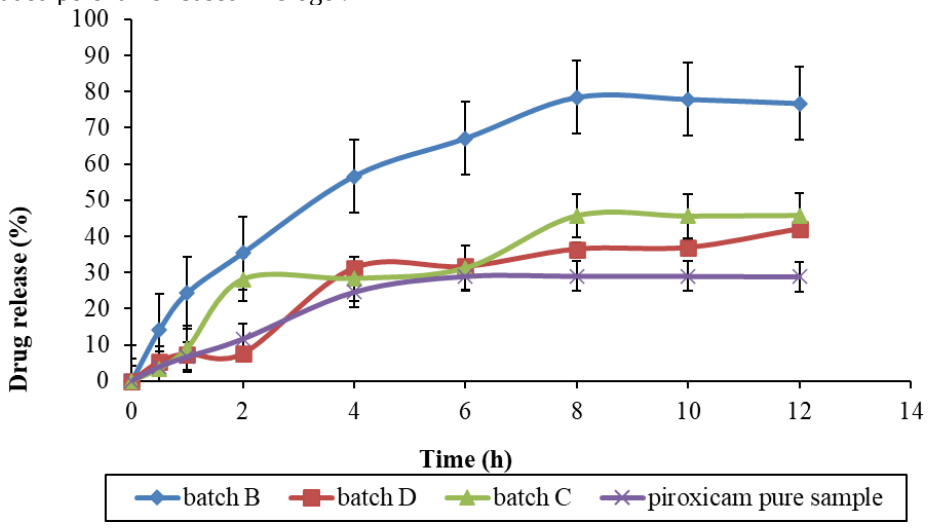

(A)

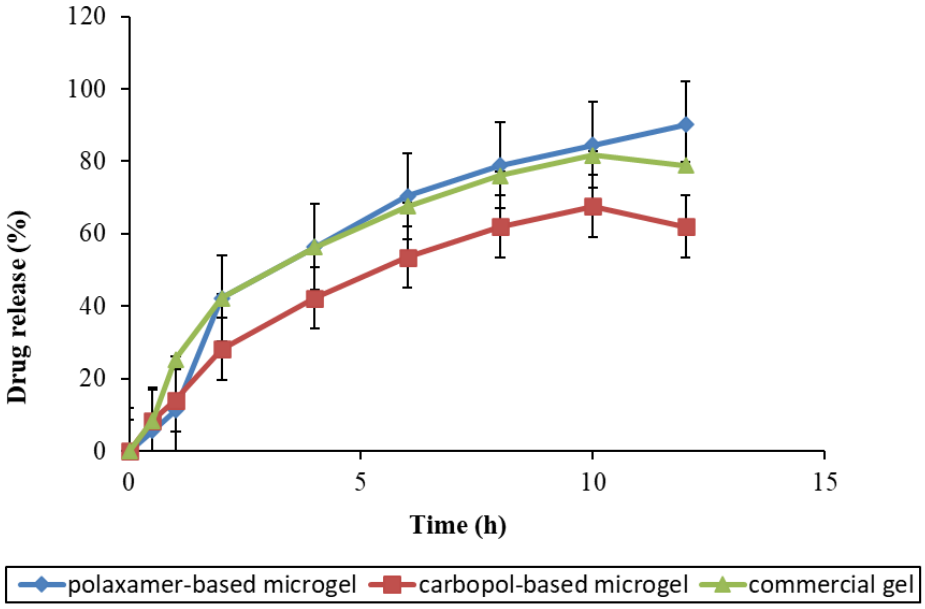

(B)

Figure 8. Release profiles of piroxicam from (A) piroxicam-loaded SLM formulation in phosphate buffer, pH 7.4, and (B) piroxicam-loaded gel formulations in phosphate buffer, pH 5.5.

Drug release from the microgels correlates with the result obtained from the viscosity and spreadability evaluations since lower viscosity could lead to higher spreadability and more effective drug release. The microgels equally served as a good platform for topical delivery of piroxicam, having recorded enhanced drug release compared with market piroxicam topical gel formulation, which is in perfect agreement with a recent study on topical microgels reported elsewhere [74].

3.4. Pharmacodynamics of the oral SLMs and topical gel formulations.

The pharmacodynamic properties of the optimized SLM and microgel formulations administered orally and topically, respectively, are correspondingly shown in Figures 9A and 9B as a function of time. The formulations exhibited edema inhibition values statistically different from controls ($p < 0.05$). Oral piroxicam-loaded surface-engineered SLMs showed high inhibition of edema (92 ± 0.7 %) in comparison with the reference drug (66 ± 0.5 %) within the 6 h test period (Figure 9A). Similarly, optimized poloxamer-based microgel exhibited 67.7 % inhibition of edema, while Carbopol-based microgels and commercial piroxicam samples exhibited 65.6 % edema inhibition after 6 h test period (Figure 9B).

Furthermore, administration of the optimized SLMs and microgels led to reduction in the edema caused by the phlogistic agent. Higher edema inhibition values obtained with optimized SLMs suggest that formulation of piroxicam as SLMs increased the bioavailability of the drug which was observed as higher therapeutic action. In addition, the increased surface area of the microgels enhanced the anti-inflammatory activity of piroxicam. Besides, the microgels formulations had sustained therapeutic action. Piroxicam stops edema by blocking the action of the cyclooxygenase enzyme which is needed for prostaglandins synthesis [2]. Optimized poloxamer-based microgel (batch B) had a slightly higher activity than the commercial piroxicam gel, which might be due to the micro-meter size of the piroxicam particle present in the microgels formulation. The reduction in particle size increased the surface area and led to increased drug permeability. Overall, the microgels formulations had

delayed anti-inflammatory activity compared to the SLMs. The pharmacodynamics of the positive control and optimized SLMs and microgels indicates a improved bioavailability of the peoral piroxicam-loaded formulations, which agrees with recent reports on lipid-based formulations of piroxicam [1-4,57].

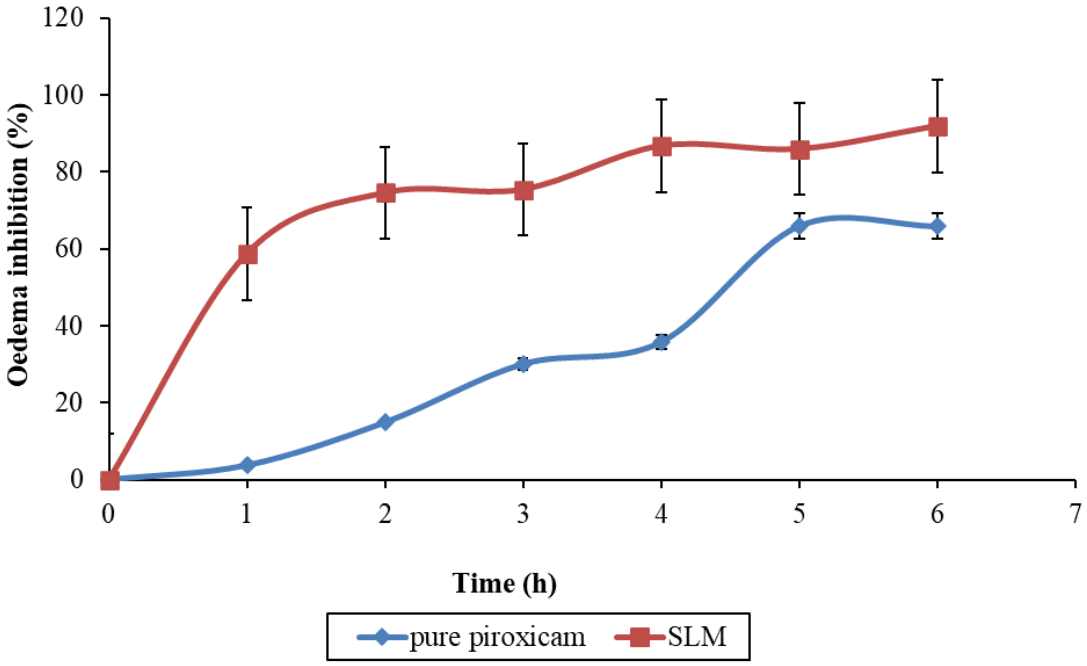

(A)

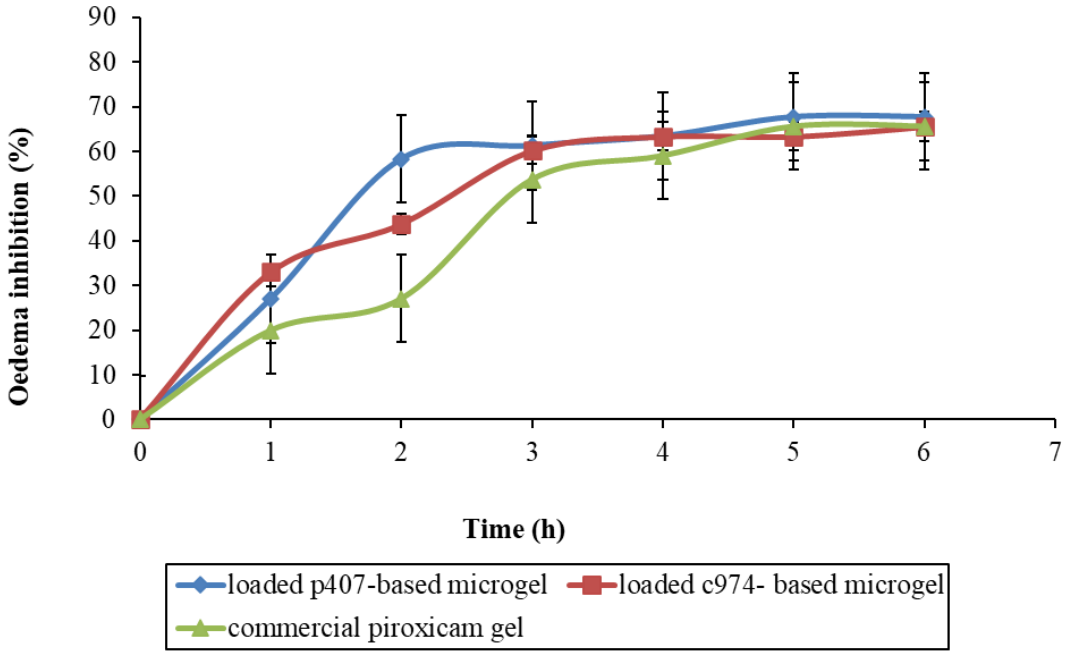

(B)

Figure 9. Inhibition of edema against time for (A) optimized piroxicam-loaded SLMs and (B) optimized piroxicam-loaded gel formulations.

4. Conclusions

In this study, formulation of piroxicam as surface-engineered oral SLMs and topical microgels based on tailor-made CH/Transcutol-HP lipid-matrix preserved the integrity of the drug and enhanced its pharmacodynamics compared with controls, an indication of enhanced

bioavailability of the optimized oral and topical lipid-based formulations. This is especially true for oral piroxicam-loaded surface-engineered SLMs, which showed high inhibition of edema (92 ± 0.7 %) compared with the reference drug (66 ± 0.5 %) within the 6h test period. Similarly, topical poloxamer-based microgels achieved slightly higher (67.7 ± 0.2 %) inhibition of inflammation within the 6 h test period than both the market piroxicam gel and Carbopol-based microgels which equally inhibited inflammation but to a lesser degree (65.6 ± 0.3 %) when compared to that produced by poloxamer-based systems. While the observed enhanced anti-inflammatory activity of optimized oral SLMs vis-à-vis unformulated piroxicam might be ascribed to increased loading efficiency caused by the lipidic and surfactant excipients and greater drug release from the formulation, the improvement of the anti-inflammatory effect of piroxicam by optimized poloxamer-based topical microgels vis-à-vis marketed gel formulation could be attributed to larger absorption surface area and lipophilic nature of the microgels, thus encouraging further development of the optimized oral SLM and topical microgel formulations.

Funding

This research received no external funding.

Acknowledgments

The authors wish to thank BASF, Ludwigshafen, Germany, and the Lubrizol Corporation, US, for the generous gift of Poloxamer® 407 and Carbopol® 974, respectively as well as JUHEL Pharmaceuticals Limited, Enugu, Nigeria, for the generous gift of Piroxicam pure sample used in this study.

Conflicts of Interest

The authors declare no conflict of interest.

References

1. Nnamani, P.O.; Attama, A.A.; Kenechukwu, F.C.; Ibezim, E.C.; Adikwu, M.U. Pharmacodynamics of piroxicam from novel solid lipid microparticles formulated with homolipids from *Bos indicus*. *Curr. Drug Deliv.* **2013**, *10*, 645-655, https://doi.org/10.2174/15672018100613112514571 2.
2. Nnamani, P.O.; Ibezim, E.C.; Attama, A.A.; Adikwu, M.U. Piroxicam-loaded P90Glylated tallow fat-based solid lipid microparticles: characterization and *in-vivo* evaluation. *Nig. J. Pharm. Res.* **2010**, *8*, 19 – 35.
3. Brown, S.A.; Chime, S.A.; Attama, A.A.; Agu, C.I.; Onunkwo, G.C. Piroxicam-loaded dika wax lipospheres: *in-vitro* and *in-vivo* characterization. *Trop. J. Pharm. Res*. **2013**, *12*, 33-38.
4. Kullich, W.; Wottawa, A.; Klein, G. Blood levels and therapeutic effectiveness of piroxicam as affected by the time of administration. *Arzeneimiltelforsching* **1985**, *35*, 1477-1479.
5. Reithmeier, H.J.; Herrmann, J.; Gopferich, A. Development and characterization of lipid microparticles as a drug carrier for somatostatin. *Int. J. Pharm*. **2001**, *218*, 133–143, https://doi.org/10.1016/s0378-5173(01)00620-2.
6. Reithmeier, H.; Hermann, J.; Gopferich, A. Lipid microparticles as a parenteral controlled release device for peptides. *J. Control. Rel*. **2001**, *73*, 339-350, https://doi.org/10.1016/s0168-3659(01)00354-6.
7. Pichayakorn, W.; Kusonwinyanwang, C.; Lakornrach, T.; Thirapakpoomanunt, S.; Lipipun, V.; Ritthidej, G.C. Solid lipid microparticles for oral Japanese encephalitis vaccine delivery: *In-vitro* study in Caco-2-cells and human intestinal M-cells models and *in-vivo* immunization in mice. *Proc. Int. Symp. Control. Rel. Bioact. Mater*. **2006**, *33*.
8. Nnamani, P.O.; Attama, A.A.; Ibezim, E.C.; Adikwu, M.U. SRMS 142-based solid lipid microparticles: Application in oral delivery of glibenclamide to diabetic rats. *Eur. J. Pharm. Biopharm*. **2010**, *76*, 68-74, https://doi.org/10.1016/j.ejpb.2010.06.002.

9. Ofokansi, K.C.; Kenechukwu, F.C.; Isah, A.B. Poloxamer-stabilized topical miconazole nitrate-loaded microemulsion: Formulation design and characterization. *J. Disp. Sci. Tech*. **2013**, *34*, 1563-1574, https://doi.org/10.1080/01932691.2012.752713.
10. Kenechukwu, F.C.; Kalu, C.F.; Momoh, M.A.; Onah, A.I.; Attama, A.A.; Okore, V.C. Novel *Bos indicus* fat-based nanoparticulate lipospheres of miconazole nitrate as enhanced mucoadhesive therapy for oral candidiasis. *Biointerface Research in Applied Chemistry*. **2023**, *13*, 1-19, https://doi.org/10.33263/BRIAC131.024.
11. Kenechukwu, F.C.; Nnamani, D.O.; Nmesirionye, B.U.; Isaac, G.T.; Momoh, M.A.; Attama, A.A. PEGylated lipid nanocontainers tailored with sunseed-oil-based solidified reverse micellar solution for enhanced pharmacodynamics and pharmacokinetics of metformin. *J. Pharm. Innov.* **2022**, 1-19, https://doi.org/10.1007/s12247-022-09654-w.
12. Kenechukwu, F.C.; Nnamani, D.O.; Duhu, J.C.; Nmesirionye, B.U.; Momoh, M.A.; Akpa, P.A.; Attama, A.A. Potential enhancement of metformin hydrochloride in solidified reverse micellar solution-based PEGylated lipid nanoparticles targeting therapeutic efficacy in diabetes treatment. *Heliyon*. **2022**, *8*, 1-16, https://doi.org/10.1016/j.heliyon.2022.e09099.
13. Kenechukwu, F.C.; Isaac, G.T.; Nnamani, D.O.; Momoh, M.A.; Attama, A.A. Enhanced circulation longevity and pharmacodynamics of metformin from surface-modified nanostructured lipid carriers based on solidified reverse micellar solutions. *Heliyon*. **2022**, *8*, 1-16, https://doi.org/10.1016/j.heliyon.2022.e09100.
14. Momoh, M.A.; Chime, S.A.; Anih, C.V.; Omeh, C.R.; Ogbonna, J.; Aminu, N.; Oyeniyi, J.; Muhammed, A.; Kenechukwu, F.C.; David, D.D. A novel formulation design based on hetero-templated solid lipid microparticles to improve solubility of anti-inflammatory piroxicam for oral administration. *New J. Chem.* **2022**, *46*, 3961-3965, https://doi.org/10.1039/D1NJ05281K.
15. Uronnachi, E.M.; Attama, A.A.; Kenechukwu, F.C.; Umeyor, C.E.; Gugu, T.H.; Nwakile, C.; Ikeotuonye, C. Solidified reverse micellar solution- (SRMS-) based microparticles for enhanced oral bioavailability and systemic antifungal efficacy of miconazole nitrate in Immunocompromised Mice. *Biomed Res. Int.* **2022**, *2022*, https://doi.org/10.1155/2022/8930709.
16. Kenechukwu, F.C.; Dias, M.L.; Eduardo Ricci-Júnior, E. Biodegradable nanoparticles from prosopisylated cellulose as a platform for enhanced oral bioavailability of poorly water-soluble drugs. *Carbohydrate Polymers*. **2021**, *256*, 1-13, https://doi.org/10.1016/j.carbpol.2020.117492.
17. Kenechukwu, F.C.; Momoh, M.A.; Nnamani, P.O.; Umeyor, C.E.; Uronnachi, E.M.; Dias, M.L.; Ibezim, E.C.; Attama, A.A. (2021). Dual-responsive micellar microgels matrixed with surface-engineered lipids: a new approach for controlled vaginal drug delivery. *J. Pharm. Innov*. **2021**, *17*, 821-839, https://doi.org/10.1007/s12247-021-09546-5.
18. Nnamani, P.O.; Kenechukwu, F.C.; Nwagwu, S.C.; Okoye, O.; Attama, A.A. Physicochemical characterization of artemether-entrapped solid lipid microparticles prepared from templated-compritol and *Capra hircus* (goat fat) homolipid. *Dhaka Univ. J. Pharm. Sci*. **2021**, *20*, 67-80, https://doi.org/10.3329/dujps.v20i1.54034.
19. Nnamani, P.O.; Ugwu, A.A.; Nnadi, O.H.; Kenechukwu, F.C.; Ofokansi, K.C.; Attama, A.A.; Lehr, C.-M. Formulation and evaluation of transdermal nanogel for delivery of artemether. *Drug Deliv. Trans. Res*. **2021**, *11*, 1655-1674, https://doi.org/10.1007/s13346-021-00951-4.
20. Kenechukwu, F.C.; Abuh, S.A.; Abuh, M.A.; Momoh, M.A.; Echezona, A.C.; Attama, A.A. Novel *Capra hircus*-based miconazole nitrate-loaded mucoadhesive nanogels for enhanced treatment of oral candidiasis. *Trop. J. Nat. Prod. Res*. **2021**, *5*, 382-388.
21. Onugwu, L.A.; Agbo, C.P.; Nwagwu, C.S.; Uzondu, S.E.; Echezona, A.C.; Ogbonna, J.D.N.; Kenechukwu, F.C.; Umeyor, C.E.; Uronnachi, E.M.; Akpa, P.A.; Momoh, M.A.; Nnamani, P.O.; Muller-Goymann, C.C.; Attama, A.A. Development of lipid-based microsuspensions for improved ophthalmic delivery of gentamicin sulphate. *Ther. Deliv*. **2021**, *12*, 1-13.
22. Ogbonna, J.D.N.; Echezona, A.C.; Nwagwu, C.S.; Agbo, C.P.; Onugwu, A.L.; Kenechukwu, F.C.; Akpa, P.A.; Momoh, M.A.; Attama, A.A. Formulation, *in vitro* and *in vivo* evaluation of sustained released artemether-lumefantrine-loaded microstructured solid lipid microparticles (SLMs). *Trop. J. Nat. Prod. Res*. **2021**, *5*, 1460-1469.
23. Onugwu, L.A.; Attama, A.A.; Nnamani, P.O.; Onugwu, S.O.; Onuigbo, E.B.; Khutoryanskjy, V.V. Development and optimization of solid lipid nanoparticles coated with chitosan and poly(2-ethyl-2-oxazoline) for ocular drug delivery of ciprofloxacin. *J. Drug Deliv. Sci. Tech*. **2022**, *74*, https://doi.org/10.1016/j.jddst.2022.103527.
24. Agbo, C.P.; Ugwuanyi, T.C.; Ugwuoke, W.I.; McConville, C.; Attama, A.A.; Ofokansi, K.C. Intranasal artesunate-loaded nanostructured lipid carriers: A convenient alternative to parenteral formulations for the treatment of severe and cerebral malaria. *J. Control Rel*. **2021**, *334*, 224–236, https://doi.org/10.1016/j.jconrel.2021.04.020.
25. Copland, M.J.; Rades, T.; Davies, N.M.; Baird, M.A. Lipid-based particulate formulations for the delivery of antigen. *Immunol. Cell Biol*. **2005**, *83*, 97-105, https://doi.org/10.1111/j.1440-1711.2005.01315.x.

26. Pandey, R.; Khuller, G.K. Solid lipid particle-based inhalable sustained drug delivery system against experimental tuberculosis. *Tuberculosis.* **2005**, *85*, 227-234, https://doi.org/10.1016/j.tube.2004.11.003.
27. Souto, E.B.; Muller, R.H.; Almeida, A.J. Topical delivery of oily actives using solid lipid particles. *Pharm. Tech*. **2007**, *19*, 28-32.
28. Passerini, N.; Gavini, E.; Albertini, B.; Rassu, G.; Di Sabatino, M.; Sanna, V.; Giunchedi, P.; Rodriguez, L. Evaluation of solid lipid microparticles produced by spray congealing for topical application of econazole nitrate. *J. Pharm. Pharmacol*. **2009**, *61*, 559-567.
29. De Jalon, E.G.; Blanco-Prieto, M.J.; Ygartua, P.; Santoyo, S. PLGA microparticles: possible vehicle for topical drug delivery. *Int. J. Pharm*. **2001**, *226*, 181-184, https://doi.org/10.1016/s0378-5173(01)00811-0.
30. Chineke, E.E.; Chime, S.A.; Kenechukwu, F.C.; Muller-Goymann, C.C.; Attama, A.A.; Okore, V.C. Formulation of novel artesunate-loaded solid lipid microparticles (SLMs) based on dika wax matrices: *in-vitro and in-vivo* evaluation. *J. Drug Deliv. Sci. Tech*. **2014**, *24*, 69-77, https://doi.org/10.1016/S1773-2247(14)50010-X.
31. Yadav, V.R.; Suresh, S.; Devi, K.; Yadav, S. Novel formulation of solid lipid microparticles of curcumin for anti-angiogenic and anti-inflammatory activity for optimization therapy of inflammatory bowel disease. *J. Pharm. Pharmacol*. **2009**, *61*, 311-321, https://doi.org/10.1211/jpp.61.03.0005.
32. Mezzena, M.; Scalia, S.; Young, P.M.; Traini, D. Solid lipid budesonide microparticles for controlled release inhalation therapy. *AAPS Pharm. Sci. Tech*. **2009**, *11*, 771-778, https://doi.org/10.1208%2Fs12248-009-9148-6.
33. Li, Y.Z.; Sun, X.; Gong, T.; Liu, J.; Zuo, J.; Zhang, Z.R. Inhalable microparticles as carriers for pulmonary delivery of thymopentin-loaded solid lipid nanoparticles. *Pharm. Res*. **2010**, *27*, 1977-86, https://doi.org/10.1007/s11095-010-0201-z.
34. Anuradha, P.; Vandana, P. Novel lipid-based systems for improved topical delivery of antioxidants. *Household and Personal Care Today* **2009**, 5-8.
35. Del Curto, M.D.; Chicco, D.; D'Antonio, M.; Ciolli, V.; Dannan, H.; D'Urso, S.; Neuteboom, B.; Pompili, S.; Schiesaro, S.; Esposito, P. Lipid microparticles as sustained release system for a GnRH antagonist (Antide). *J. Control. Rel.* **2003**, *89*, 297-310, https://doi.org/10.1016/s0168-3659(03)00120-2.
36. Joshi, N.H.; Shah, N. Review of lipids in pharmaceutical drug delivery system, Part I. *Amer. Pharm. Rev*. **2008**, *1*, 27-38.
37. Friedrich, I.; Papantoniou, I.; Müller-Goymann, C.C. Physicochemical characterization of a reverse micellar solution after loading with different drugs. *Pharmazie*. **2000**, *55*, 755-8.
38. Friedrich, I,; Müller-Goymann, C.C. Characterization of solidified reverse micellar solutions (SRMS) and production development of SRMS-based nanosuspensions. *Eur. J. Pharm. Biopharm*. **2003**, *56*, 111-9, https://doi.org/10.1016/s0939-6411(03)00043-2.
39. Friedrich, I.; Reichl, S.; Müller-Goymann, C.C. Drug release and permeation studies of nanosuspensions based on solidified reverse micellar solutions (SRMS). *Int. J. Pharm*. **2005**, *305*, 167-75, https://doi.org/10.1016/j.ijpharm.2005.09.007.
40. Umeyor, C.E.; Kenechukwu, F.C.; Ogbonna, J.D.N.; Chime, S.A.; Attama, A.A. Investigation of solidified reverse micellar systems as novel carriers for oral delivery of gentamicin. *J. Pharm. Res*. **2012**, *5*, 4914-20.
41. Kenechukwu, F.C.; Umeyor, C.E.; Momoh, M.A.; Ogbonna, J.D.N.; Chime, S.A.; Nnamani, P.O.; Attama, A.A. Evaluation of gentamicin-entrapped solid lipid microparticles formulated with a biodegradable homolipid from *Capra hircus*. *Trop. J. Pharm. Res*. **2014**, *13*, 1999-1205.
42. Kenechukwu, F.C.; Momoh, M.A.; Nnamani, P.O.; Attama, A.A. Solid lipid micro-dispersions (SLMs) based on PEGylated solidified reverse micellar solutions (SRMS): a novel carrier system for gentamicin. *Drug Deliv*. **2015**, *22*, 710-722, https://doi.org/10.3109/10717544.2014.900152.
43. Momoh, M.A.; Kenechukwu, F.C.; Attama, A.A. Formulation and evaluation of novel solid lipid microparticles as a sustained release system for the delivery of metformin hydrochloride. *Drug Deliv*. **2013**, *20*, 102–111, https://doi.org/10.3109/10717544.2013.779329.
44. Kenechukwu, F.C.; Momoh, M.A.; Nnamani, P.O.; Ogbonna, J.D.N.; Umeyor, C.E.; Attama, A.A. Improved bioactivity of gentamicin from novel solid lipid microparticles based on beeswax. *Nig. J. Pharm. Res*. **2014**, *10*, 35-45.
45. Chime, S.A.; Attama, A.A.; Kenechukwu, F.C.; Umeyor, E.C.; Onunkwo, G.C. Formulation, *in-vitro* and *in-vivo* characterisation of diclofenac potassium sustained release tablets based on solidified reverse micellar solution (SRMS). *British J. Pharm. Res.* **2013**, *3*, 90-107.
46. Umeyor, E.C.; Kenechukwu, F.C.; Ogbonna, J.D.; Chime, S.A.; Attama, A.A. Preparation of novel solid lipid microparticles loaded with gentamicin and its evaluation *in-vitro* and *in-vivo*. *J. Microencapsul*. **2012**, *29*, 296–307, https://doi.org/10.3109/02652048.2011.651495.
47. Kenechukwu, F.C.; Umeyor, C.E.; Ogbonna, J.D.N.; Builders, P.F.; Attama, A.A. Preliminary studies on the functional properties of gentamicin in SRMS-based solid lipid microparticles. *Int. J. Novel Drug Deliv. Tech*. **2011**, *1*, 130-142.
48. Nnamani, P.O.; Ibezim, E.C.; Attama, A.A.; Adikwu, M.U. Surface-modified solid lipid microparticles based on homolipids and Softisan® 142: Preliminary characterization. *Asian Pac. J. Trop. Med.* **2010**, *3*, 205–210.

49. Nnamani, P.O.; Ibezim, E.C.; Attama, A.A.; Adikwu, M.U. New approach to solid lipid microparticles using biocompatible homolipids-templated heterolipid microcarriers for cimetidine delivery. *Nig. J. Pharm. Res.* **2010**, *8*, 92–111.
50. Chime, S.A.; Attama, A.A.; Obitte, N.C.; Kenechukwu, F.C.; Agubata, C.O.; Ezekwe, C.C. *In-vitro* and *in-vivo* characterisation of indomethacin-loaded dika fat-based solid lipid microparticles. *Int. J. Pharm. Sci. Rev. Res.* **2012**, *16*, 10-16.
51. Jaspart, S.; Bertholet, D.L.; Evrard, B. Study of solid lipid microparticles as sustained release delivery system for pulmonary administration. 15th Int. Symp. on Microencapsul. Parma, Italy, **2005**.
52. Kumar, M.N.V.R. Nano and microparticles as controlled drug delivery devices. *J. Pharm. Pharm. Sci.* **2000**, *3*, 234–258.
53. Attama, A.A.; Müller-Goymann, C.C. Effect of beeswax modification on the lipid matrix and solid lipid nanoparticle crystallinity. *Colloids and Surfaces A: Physicoch. & Eng. Aspects* **2008**, *315*, 189-195, https://doi.org/10.1016/j.colsurfa.2007.07.035.
54. Attama, A.A.; Schicke, B.C.; Müller-Goymann, C.C. Novel physically structured lipid matrices of beeswax and a homolipid from *Capra hircus* (goat fat): A physicochemical characterization. *J. Drug Deliv. Sci. Technol*. **2007**, *17*, 103-112, https://doi.org/10.1016/S1773-2247(07)50016-X.
55. Attama, A.A.; Schicke, B.C.; Paepenmüller, T.; Müller-Goymann, C.C. Solid lipid nanodispersions containing mixed lipid core and a polar heterolipid: Characterization. *Eur. J. Pharm. Biopharm.* **2007**, *67*, 48-57, https://doi.org/10.1016/j.ejpb.2006.12.004.
56. Attama, A.A.; Müller-Goymann, C.C. Investigation of surface-modified solid lipid nanocontainers formulated with a heterolipid-templated homolipid. *Int. J. Pharm*. **2007,** *334*, 179-189, https://doi.org/10.1016/j.ijpharm.2006.10.032.
57. Attama, A.A.; Mpamaugo, V.E. Pharmacodynamics of piroxicam from self-emulsifying lipospheres formulated with homolipids extracted from *Capra hircus*. *Drug Deliv*. **2006**, *13*, 133-137, https://doi.org/10.1080/10717540500313430.
58. Attama, A.A.; Nkemnele, M.O. *In-vitro* evaluation of drug release from self micro-emulsifying drug delivery systems using a novel biodegradable homolipid from *Capra hircus*. *Int. J. Pharm*. **2005**, *304*, 4-10, https://doi.org/10.1016/j.ijpharm.2005.08.018.
59. Kenechukwu, F.C.; Momoh, M.A.; Umeyor, C.E.; Uronnachi, E.M.; Attama, A.A. Investigation of novel solid lipid microparticles based on homolipids from *Bos indicus* for the delivery of gentamicin. *Int. J. Pharma Investig*. **2016**, *6*, 32–38, https://doi.org/10.4103/2230-973x.176473.
60. Nnamani, P.O.; Kenechukwu, F.C.; Dibua, E.U.; Ogbonna, C.C.; Momoh, M.A.; Olisemeke, A.U.; Agubata, C.O.; Attama, A.A. Formulation, characterization and *ex-vivo* permeation studies on gentamicin-loaded transdermal patches based on PURASORB® polymers. *Sci Res Essays.* **2013**, *8*, 973–982.
61. Nnamani, P.O.; Kenechukwu, F.C.; Dibua, E.U.; Ogbonna, C.C.; Momoh, M.A.; Ogbonna, J.D.N.; Okechukwu, D.C.; Olisemeke, A.U.; Attama, A.A. Bioactivity of gentamicin contained in novel transdermal drug delivery systems (TDDS) formulated with biodegradable polyesters. *Afr. J. Pharm. Pharmacol*. **2013**, *7*, 1987–1993.
62. Allen, L.V. Transdermals: the skin as part of a drug delivery system. *Int. J. Pharm. Compound.* **2011**, *15*, 308–315, https://doi.org/10.3390%2Fpharmaceutics7040438.
63. Prausnitz, M.R.; Langer, R. Transdermal drug delivery. *Nat. Biotechnol*. **2008**, *26*, 1261–1268, https://doi.org/10.1038/nbt.1504.
64. Azarmi, R.; Roa, W.; Löbenberg, R. Current perspectives in dissolution testing of conventional and novel dosage forms. *Int. J. Pharm*. **2007**, *328*, 12–21, https://doi.org/10.1016/j.ijpharm.2006.10.001.
65. Nnamani, P.O.; Kenechukwu, F.C.; Dibua, E.U.; Ogbonna, C.C.; Monemeh, U.L.; Attama, A.A. Transdermal microgels of gentamicin. *Eur. J. Pharm. Biopharm*. **2013**, *84*, 345-354, https://doi.org/10.1016/j.ejpb.2012.11.015.
66. Nnamani, P.O.; Kenechukwu, F.C.; Anugwolu, C.L.; Attama, A.A. Evaluation of hydrogels based on poloxamer 407 and polyacrylic acids for enhanced topical activity of gentamicin against susceptible infections. *Trop. J. Pharm. Res.* **2014**, *13*, 1385-1391, http://dx.doi.org/10.4314/tjpr.v13i9.2.
67. Nnamani, P.O.; Kenechukwu, F.C.; Anugwolu, C.L.; Agubata, C.O.; Attama, A.A. Characterization and controlled release of gentamicin from novel hydrogels based on poloxamer 407 and polyacrylic acids. *Afr. J. Pharm. Pharmacol*. **2013**, *7*, 2540–2552, http://dx.doi.org/10.5897/AJPP2013.3803.
68. Nnamani, P.O.; Dibua, E.U.; Kenechukwu, F.C.; Ogbonna, C.C.; Onyemaechi, C.; Attama, A.A. Novel lipid-based dermal microgels of Neobacin®. *Afr. J. Biotechnol*. **2015**, *14*, 979-989.
69. Levintova, Y.; Plakogiannis, F.M.; Bellantone, R.A. An improved *in-vitro* method for measuring skin permeability that controls excess hydration of skin using modified Franz diffusion cells. *Int. J. Pharm.* **2001**, *419*, 96–106, https://doi.org/10.1016/j.ijpharm.2011.07.025.
70. Umeyor, C.; Attama, A.; Uronnachi, E.; Kenechukwu, F.; Nwakile, C.; Nzekwe, I.; Okoye, E; Esimone, C. Formulation design and *in-vitro* physicochemical characterization of surface-modified self-nanoemulsifying formulations (SNEFs) of gentamicin. *Int. J. Pharm*. **2016**, *497*, 161-198, https://doi.org/10.1016/j.ijpharm.2015.10.033.

71. Obitte, N.C.; Ofokansi, K.C.; Kenechukwu, F.C. Development and evaluation of novel self-nanoemulsifying drug delivery systems based on a homolipid from *Capra hircus* and its admixtures with melon oil for the delivery of indomethacin. *J. Pharm*. **2014**, *2014*, 1-10, https://doi.org/10.1155/2014/340486.
72. Souto, E.B.; Doktorovova, S.; Boonme, P. Lipid-based colloidal systems (nanoparticles, microemulsions) for drug delivery to the skin: materials and end-product formulations. *J. Drug Del. Sci. Tech*. **2011**, *21*, 43-54, https://doi.org/10.1016/S1773-2247(11)50005-X.
73. Joseph, N.; Lakshims, L.; Jayakrishnan, A. A floating–type oral dosage form for piroxicam based on hollow polycarbonate microspheres; *in-vitro* and *in-vivo* evaluation in rabbits. *J. Control. Rel*. **2002**, *79*, 71–79, https://doi.org/10.1016/s0168-3659(01)00507-7.
74. Kenechukwu, F.C.; Attama, A.A.; Ibezim, E.C.; Nnamani, P.O.; Umeyor, C.E.; Uronnachi, E.M.; Gugu, T.H.; Momoh, M.A.; Ofokansi, K.C.; Akpa, P.A. Surface-modified mucoadhesive microgels as a controlled release system for miconazole nitrate to improve localized treatment of vulvovaginal candidiasis. *Eur. J. Pharm. Sci*. **2018**, *111*, 358–375, https://doi.org/10.1016/j.ejps.2017.10.002.